# Dendritic spines are lost in clusters in patients with Alzheimer's disease

Mite Mijalkov[1], Giovanni Volpe[2], Isabel Fernaud-Espinosa[3,4], Javier DeFelipe[3,4,5], Joana B. Pereira[1, 6, #, *] and Paula Merino-Serrais[3, 4, #, *]

[1]Department of Neurobiology, Care Sciences and Society, Karolinska Institutet, Stockholm, Sweden

[2]Department of Physics, Goteborg University, Goteborg, Sweden

[3]Laboratorio Cajal de Circuitos Corticales (CTB), Universidad Politécnica de Madrid, Madrid, Spain.

[4]Departamento de Neurobiología Funcional y de Sistemas, Instituto Cajal, CSIC, Madrid, Spain.

[5]Centro de Investigación Biomédica en Red sobre Enfermedades Neurodegenerativas (CIBERNED), ISCIII, Madrid, Spain

[6]Memory Research Unit, Department of Clinical Sciences, Malmö, Lund University, Lund, Sweden

[#] P. Merino-Serrais and Joana B. Pereira share the last position as senior authors in this work.

* Corresponding authors:

Paula Merino-Serrais. Laboratorio Cajal de Circuitos Corticales, Centro de Tecnología Biomédica, Universidad Politécnica de Madrid, Campus Montegancedo S/N, Pozuelo de Alarcon, 28223 Madrid // Instituto Cajal (CSIC), Avenida Doctor Arce, 37, 28002 Madrid, Spain. Tel: (+34) 910679292 // paula.merino-serrais@cajal.csic.es

Joana B. Pereira. Department of Neurobiology, Care Sciences and Society, Karolinska Institutet, Stockholm, Sweden // Memory Research Unit, Department of Clinical Sciences, Malmö, Lund University, Lund, Sweden. Tel: (+46) 70 99 66 186 // joana.pereira@ki.se

**SUMMARY**

Alzheimer's disease (AD) is a progressive neurodegenerative disorder characterized by a deterioration of neuronal connectivity. The pathological accumulation of tau protein in neurons is one of the hallmarks of AD and has been connected to the loss of dendritic spines of pyramidal cells, which are the major targets of cortical excitatory synapses and key elements in memory storage. However, the detailed mechanisms underlying the loss of dendritic spines in patients with AD are still unclear. Here, comparing dendrites with and without tau pathology of AD patients, we show that the presence of tau pathology determines the loss of dendritic spines in blocks, ruling out alternative models where spine loss occurs randomly. Since memory storage has been associated with synaptic clusters, the present results provide a new insight into the mechanisms by which tau drives synaptic damage in AD, paving the way to memory deficits by altering spine organization.

## INTRODUCTION

Alzheimer's disease (AD) is the most common neurodegenerative disorder; it is characterized by a progressive loss of memory, followed by decline in other cognitive functions and ultimately dementia [1]. These clinical symptoms are thought to be caused by the underlying pathological processes associated with AD, in particular, the aggregation of tau protein into neurofibrillary tangles and the loss of crucial structures for synaptic communication such as dendritic spines (for simplicity, spines) [2]. However, the mechanisms that link tau pathology to spine loss in AD patients are currently unclear. Clarifying their relation is nevertheless important to improve our understanding of the pathophysiology of AD and to develop future treatment strategies that target more specifically these mechanisms.

Amongst the wide range of neural cells forming the human brain, pyramidal neurons are particularly important because they are the most abundant neurons and connect different areas of the neocortex, the hippocampus and the amygdala [3]. Previous studies have shown that changes in the spines of pyramidal neurons affect the number of excitatory inputs that these neurons receive and, consequently, the underlying cognitive processes they support, including memory and learning [3-6]. Moreover, there is evidence that the spines of pyramidal neurons are not uniformly distributed along their dendrites and can undergo specific plastic changes in their size and spatial location [7]. In particular, the activity of one spine can modulate the plasticity of neighboring spines through the mutual sharing of plasticity-related proteins or through the activation of synchronized synaptic inputs [8]. These changes occur across different time scales and typically result in the spatial organization of spines into groups or clusters. This phenomenon is known as the "clustered plasticity hypothesis" [9-12] and suggests that spines do not act as single functional units but are part of a complex network that organizes spines in groups to optimize the connectivity patterns between dendrites and surrounding axons. To this date, no studies have assessed how spine organization is affected by tau pathology in AD. Such assessment could provide an important insight into the mechanisms underlying synaptic degeneration and cognitive decline.

The aim of this study is to define the patterns of spine loss in hippocampal pyramidal neurons with tau (Tau+) and without tau (Tau-) pathology in patients with AD. From each patient, dendrites with and without tau (Tau+ and Tau- dendrites, respectively) are obtained from the pyramidal neurons of the *Cornu Ammonis* 1 (CA1), a hippocampal subfield that is crucial for memory, one of the first cognitive functions that becomes impaired in AD [13]. Building on previous evidence showing that spines are organized in groups [14], we hypothesize that the pathological changes occurring in AD do not target single spines at random locations along the dendrite, but instead damage clusters of spines that are close to each other. To test this hypothesis, we use an approach based on graph theory, where we model each dendrite as an ensemble of nodes connected by edges, where the nodes correspond to spines and the edges represent physical closeness between them (i.e., the inverse distance between the spines along the dendrite). Comparing the organization of the spines in Tau+ and Tau- dendrites, we observe that Tau+ dendrites feature smaller and shorter communities of spines, which are associated with a loss of spines. To understand the mechanism of damage leading to these differences, we perform simulated attacks on the Tau- dendrites by removing their spines according to different statistics, corresponding to a loss of spines at random or clustered locations. Our findings indicate that only by removing spines in clusters, the spine communities of the Tau- dendrites become similar to those of the Tau+ dendrites. We can therefore conclude that spines are lost in clusters in patients with AD.

## RESULTS

**Classification of Tau+ and Tau- dendrites.** Nineteen hippocampal CA1 neurons from 3 patients with AD are included in this study. These neurons are injected with Lucifer yellow (LY) fluorescent dye and immunostained with AT8 (PHF-tau$_{AT8}$) and PHF-1 tau (PHF-tau$_{PHF\text{-}1}$) antibodies [13, 15] in order to detect paired helical filaments (PHF) indicative of tau pathology [16]. The neurons immunostained by either PHF-tau$_{AT8}$ or PHF-tau$_{PHF\text{-}1}$ are classified as Tau+ dendrites, whereas those not immunostained by either of these antibodies are classified as Tau- dendrites. Only neurons in an intermediate stage of PHF-tau aggregation are included in the current study since there are virtually no spines in advanced PHF-tau stages [13].

Moreover, dendrites in contact with amyloid-beta plaques are also excluded from the analyses because the plaques are known to induce morphological alterations in neurites and spines, decreasing spine density [17-19]. Figure 1 shows examples of a Tau- neuron (Figs. 1A-C) and a Tau+ neuron (Figs. 1D-F) with zoomed-in views of their dendrites and spines (Figs. G-J). A high-resolution segment of one dendrite is depicted (Fig. 1K) with the red points indicating the measurement of number of spines on the dendrite axis (Fig. 1L) and the coordinates that are exported to build the graph representations of the same dendrite (Fig. 1M). In total, 28 dendrites are examined in the present study, of which 10 are Tau- with a total of 4628 spines, and 18 are Tau+ with a total of 8284 spines.

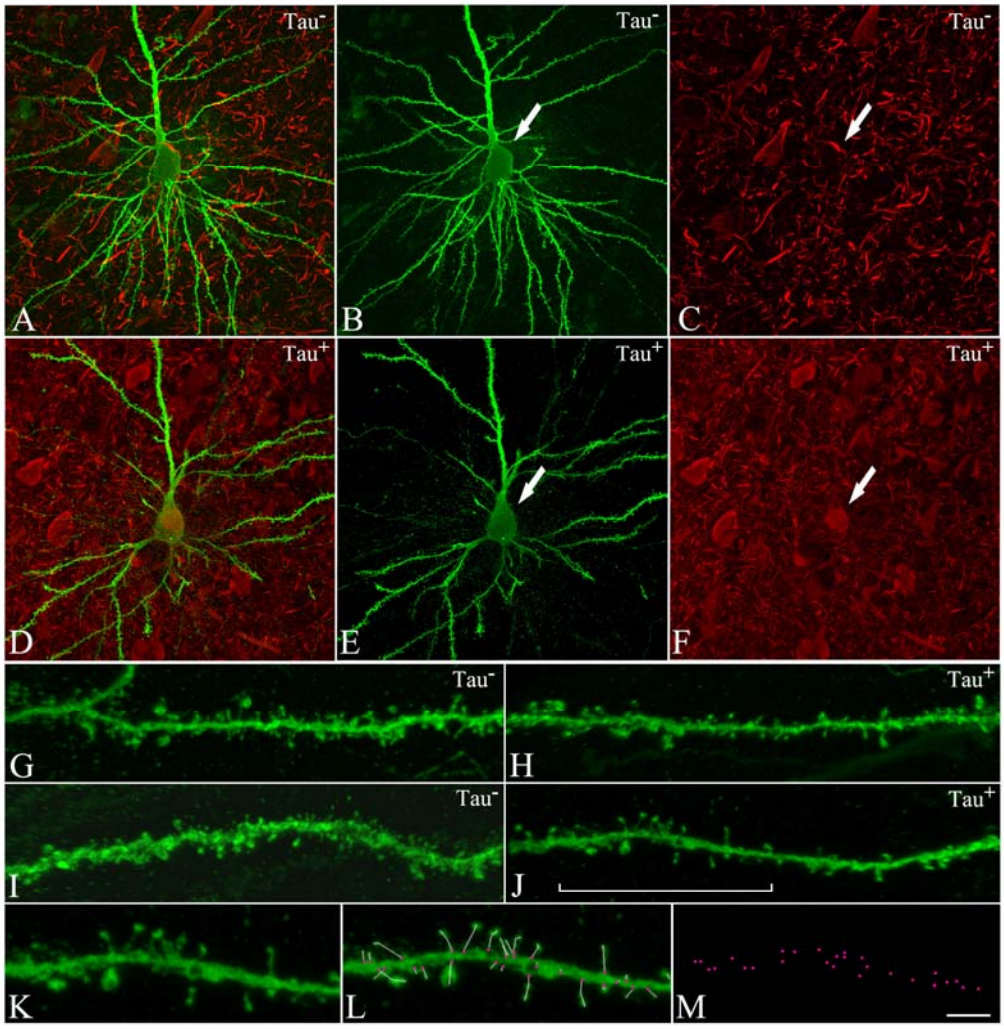


**Figure 1. CA1 pyramidal neurons with and without tau pathology.**

Confocal microscopy pictures obtained after combining the channels acquired separately for Lucifer yellow (green) and PHF-tau AT8 (red), showing (**A-F**) neurons and (**G-J**) their basal dendrites, (**A-C, G-H**) with a soma free of PHF-tau AT8 (Tau-) and (**D-F, I-J**) with PHF-tau AT8 in an intermediate stage of neurofibrillary pathology (Tau+). The position of the soma is indicated with an arrow in B-C and E-F. (**K**) High resolution image of a dendritic segment indicated with a bracket in J. (**L**) The same representative image as in K showing all the spines along the dendrite marked with a white line and pink dots for their insertion points. (**M**) 3D spatial distribution of all spines insertion points. Scale bar shown in M indicates 12 µm in A-F, 5 µm in G-J, and 3 µm in K-M.

**Tau pathology is associated with smaller and shorter communities of spines**. To evaluate whether the spines form closely connected communities, we model each dendrite as a graph, i.e., a group of nodes connected by edges. In this graph, the spines are the nodes and the edges are the connection strength between the spines. In Figure 2, we show a tree-dimensional visual representation of the spines along a dendrite (Fig. 2A) and how we calculate the connection strength between the spines, which is proportional to their physical closeness and can be measured as the inverse distance between the spines along the dendrite (Fig. 2B). The resulting graph can be represented as an adjacency matrix (Fig. 2C), where each element in the matrix represents the connection strength between the nodes in the corresponding row and column.

We define a community as a group of spines that are tightly connected with each other and poorly connected with other groups of spines along the dendrite. Therefore, we calculate the communities by dividing the dendrite into sets of spines such that the spines belonging to each set are nearer to each other compared to other spines on the dendrite. The communities are defined using the Louvain algorithm [20]. Since this algorithm has an inherent randomness, the results are averaged over 100 community structure calculations.

In Fig. 3A we show a visual representation of an example of spine communities on a dendrite, which are visually separated into three distinct color-coded communities. We also show the corresponding adjacency matrix, where the three communities can be identified as blocks of connections. In Fig. 3B, we show the community structure for one of the Tau- dendrites assessed in the current study. The community structure of each dendrite can be characterized by calculating the characteristic spread between the spines within the community (characteristic community extension, CCE, shown in Fig. 3C) and the average number of spines in each community (community size, shown in Fig. 3E). This analysis shows that the characteristic extension as well as the size of the communities are significantly smaller in Tau+ compared to Tau- dendrites (CCE: $CCE_{\text{Tau+}}$ = 20.07 ± 4.96 μm, $CCE_{\text{Tau-}}$ = 25.74 ± 5.88 μm, $p < 0.009$, Fig. 3D; community size: $N_{\text{Tau+}}$ = 47.94 ± 17.20 spines, $N_{\text{Tau-}}$ = 63.86 ± 19.71 spines, $p < 0.035$, Fig. 3F), suggesting that the spines of Tau+ dendrites are organized in smaller and more tightly packed communities compared to those of the Tau- dendrites.

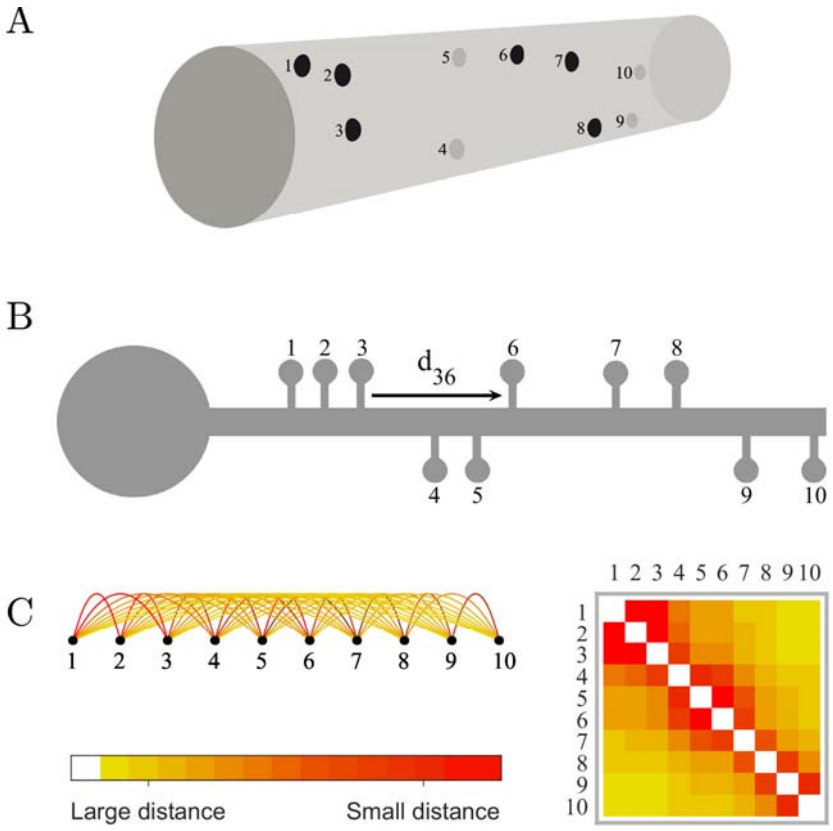


**Figure 2. Dendrites as graphs.**

(**A**) 3D Visual representation of the spines (1 to 10) along a dendritic segment . (**B**) Calculation of the connection strength between pairs of spines, which is proportional to their physical closeness and can be measured as the inverse distance between the spines along the dendrite (e.g., $d_{36}$ is the distance between spines 3 and 6, and the respective connection strength is $1/d_{36}$). (**C**) The resulting graph can be represented as an adjacency matrix, where each element in the matrix represents the strength of the connection between the nodes in the corresponding row and column.

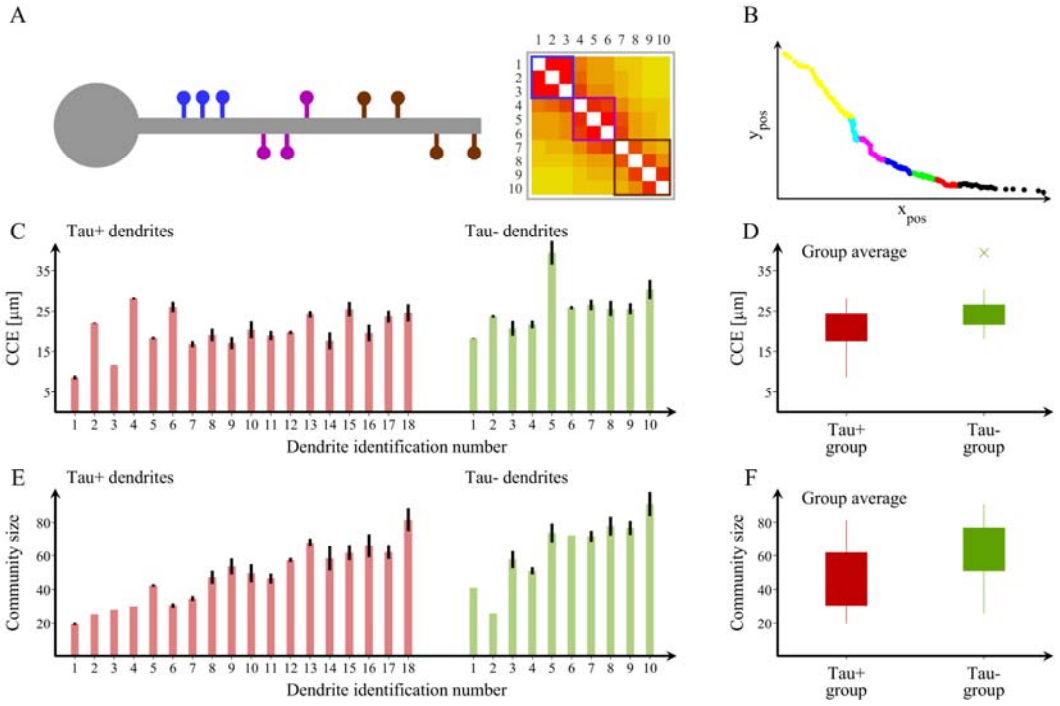


**Figure 3. Spine organization into communities.**

(**A**) Schematic representation of a dendrite with spines that can be clearly separated into three distinct communities and their corresponding adjacency matrix showing the blocks of connections that correspond to each community. (**B**) We also show an example of a community structure for one of the dendrites assessed in the current study with seven communities. The community structure is assessed using the average distance between spines that belong to each community (characteristic community extension, CCE) and the number of spines in each community. (**C, E**) We show the values obtained in these two measures for each Tau+ (red, n= 18) and Tau- (green, n = 10) dendrite, which are computed by calculating the community structure over 100 trials. In addition, we include (**D**) boxplots with the group averages for the CCE and (**F**) the average community size or number of spines for each community, which are both smaller in Tau+ compared to Tau- dendrites. The bottom and the top edges of the boxplots denote the 25$^{th}$ and 75$^{th}$ percentiles of the data, respectively. The whiskers extend to the largest and smallest data points that are not considered outliers. The outliers are plotted with the "x" symbol. The results are similar after excluding the outlier.

To further investigate this distinctive pattern of organization characterized by smaller and more tightly packed communities of spines in Tau+ dendrites compared to Tau- dendrites, we conduct two additional analyses. In the first analysis, we assess whether this organization can be explained by the loss of spines associated with tau pathology, a phenomenon that we have already reported in AD [13]. This analysis shows that the Tau+ dendrites have a significantly lower number of spines compared to their Tau- counterparts (Tau+ = 352.5 ± 106.7, Tau- = 462.8 ± 145.6, $p<0.029$, Fig. 4A, 4B, Supplementary Table 1), in line with our previous findings [13]. In the second analysis, we assess whether Tau+ dendrites have a different number of groups of spines that are closely connected with each other, which we refer to as mean grouping coefficient. This analysis shows that Tau+ dendrites have significantly higher mean grouping coefficient (Tau+ = 0.013 ± 0.004, Tau- = 0.010 ± 0.003, $p < 0.001$, Fig. 4C, 4D), indicating that their spines are organized in more isolated groups along the dendrite, whereas the Tau- dendrites have spines that are more evenly spread along the dendrite.

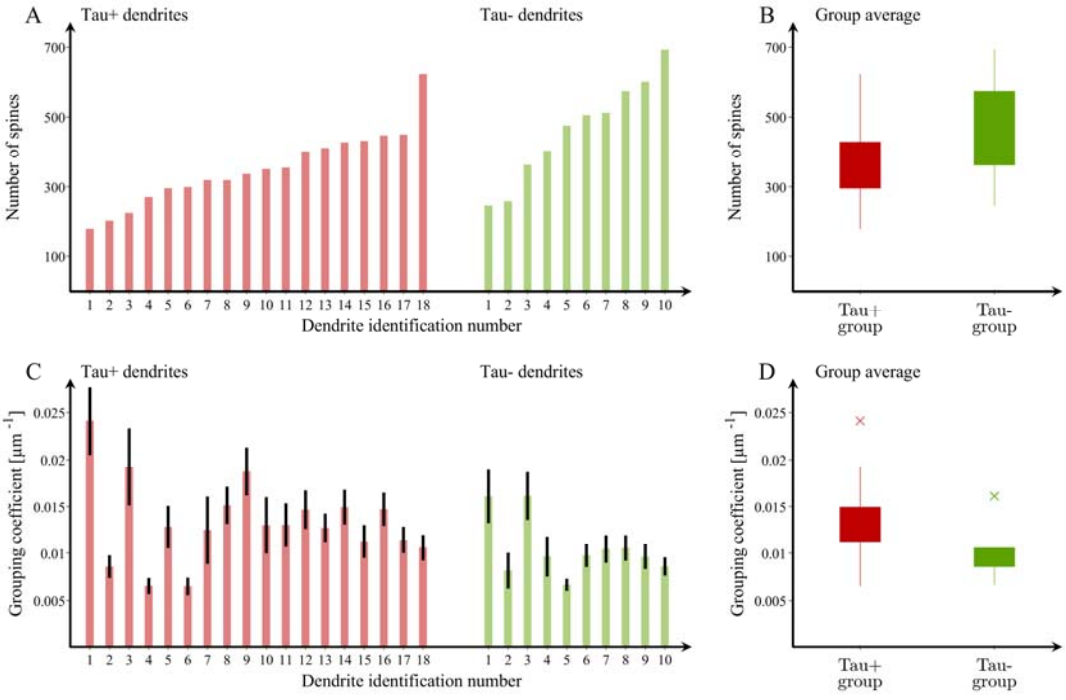


**Figure 4. Number of individual spines and mean grouping coefficient in dendrites with and without tau pathology.**

(**A**) Number of spines in the individual dendrites with tau pathology (Tau+) (n = 18; red) and without tau pathology (Tau-) (n = 10; green). Boxplots with the mean number of spines and their standard deviations in the Tau- and Tau+ dendrites. (**B**) The permutation analyses show a higher number of spines in the Tau- compared to the Tau+ group ($p = 0.029$). (**C**) Mean grouping coefficient in each individual Tau+ (n = 18; red) and Tau- (n = 10; green) dendrite. Boxplots with the mean grouping coefficients in the Tau- and Tau+ dendrites. (**D**) The permutation analyses show a higher mean grouping coefficient in the Tau+ compared to the Tau- group ($p < 0.001$). In all boxplots, their bottom and the top edges denote the $25^{th}$ and $75^{th}$ percentiles of the data, respectively. The whiskers extend to the largest and smallest data points that are not considered outliers. The outliers are plotted with the "x" symbol. The results are similar after excluding the outliers.

**The organization of Tau- dendrites becomes similar to Tau+ dendrites when clusters of spines are removed**. To investigate the mechanisms underlying the more clearly outlined communities and higher number of spine groups in the Tau+ dendrites compared to Tau- dendrites, we performed a series of simulated attacks on the Tau- dendrites by progressively removing their spines. We consider three possible attack strategies and assess their effects on the characteristic community extension as well as on the mean grouping coefficient. These attack strategies are summarized in Fig. 5A, 5D, and 5G as well as Fig. 6A, 6D and 6G. First, we perform a random attack, by removing multiple individual spines at random locations along the dendrite (Fig. 5A, 6A). Second, we perform attacks of blocks of 3 spines, where we remove groups of 3 adjacent spines at random locations along the dendrite (i.e., we select random spines for removal and we remove them together with their first-degree neighbors, Fig. 5D, 6D). Finally, we perform attacks of blocks of 5 spines, where we remove groups of 5 adjacent spines (i.e., we remove randomly selected spines together with their first- and second-degree neighbors, Fig. 5G, 6G). Due to the element of randomness in these attacks, we average our results over 100 independent attacks on each dendrite to obtain statistically reliable results.

These analyses show that removing random individual spines from the dendrite has no effect on the communities and groups of spines, even when a large number of spines is removed (Fig. 5B, 5C, 6B, 6C). In contrast, when the spines are removed in blocks of 3 or 5, the attacked Tau- dendrites show a smaller characteristic community extension (Fig. 5E-5I, Supplementary Table 2) and a greater number of groups denoted by increases in the mean grouping coefficient (Fig. 6E-6I, Supplementary Table 3), similarly to the Tau+ dendrites. These analyses indicate that the mechanism underlying the distinct organization pattern in dendrites with tau pathology entails the loss of blocks of spines.

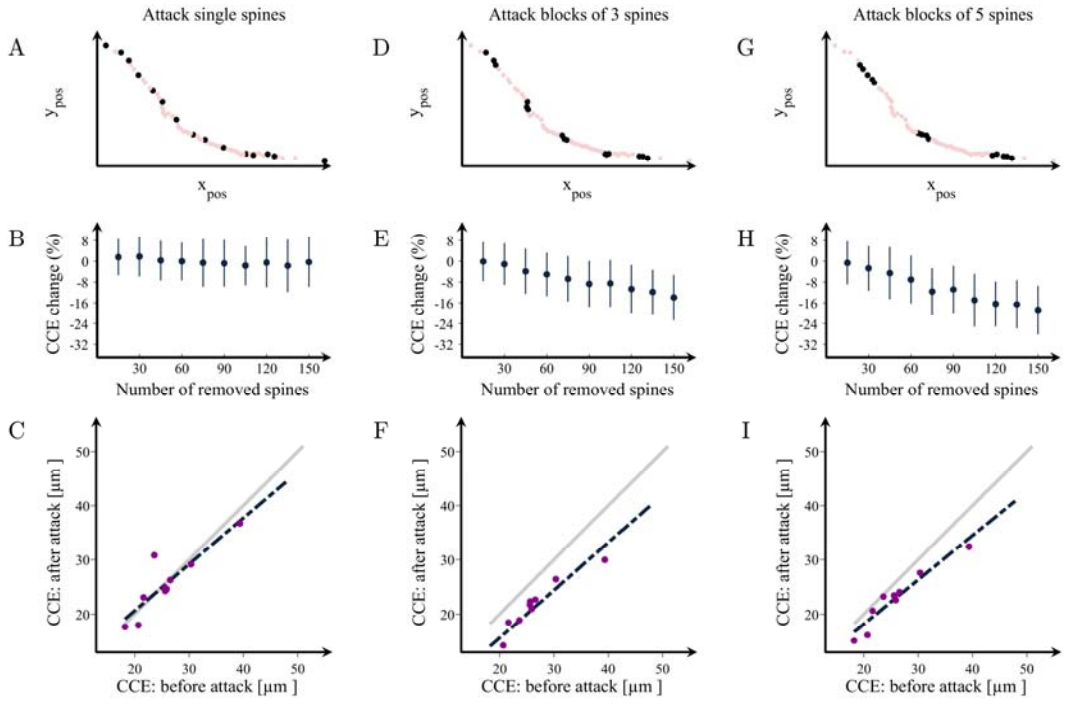


**Figure 5. Changes in the organization of dendritic spines after attacks.** Examples of attacks on spines in a representative dendrite at (**A**) random locations or in clusters of (**D**) 3 and (**G**) 5 spines. (**B, E, H**) Percentage change in the characteristic community extension (CCE) as a function of the number of removed spines in the three cases, respectively. CCE in the attacked vs. the non-attacked dendrites after the removal of 150 spines in groups of (**C**) 1, (**F**) 3 and (**I**) 5. The grey line shows the theoretical line of no change in the CCE, while the black line is the line that best fits the observed attack data. The values obtained after each attack can also be found in Supplementary Table 2. Means and standard deviations are computed over 100 random attacks.

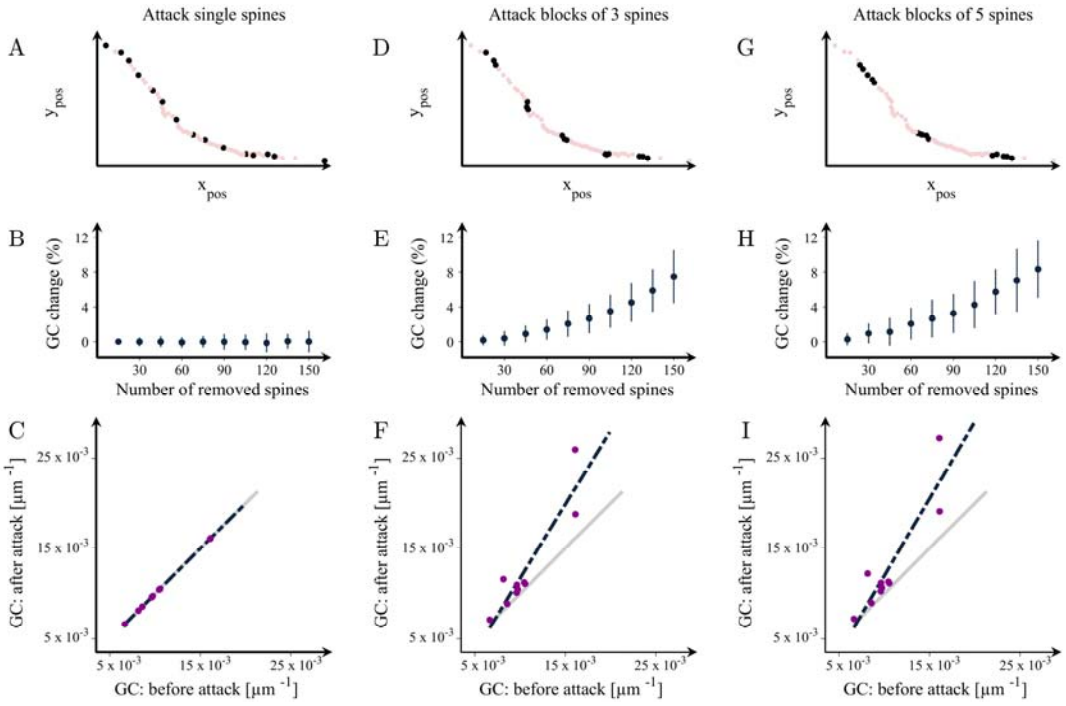


**Figure 6. Changes in the mean grouping coefficient after random attacks of spines in healthy dendrites.** Illustration of attacks on random spines in a representative dendrite in groups of (**A**) 1, (**D**) 3 and (**G**) 5. (**B, E, H**) Percentage increases in the mean grouping coefficient (GC) in that dendrite as a function of the number of removed spines in the three cases respectively. Mean grouping coefficient of the attacked vs. healthy dendrites after the removal of 150 spines in groups of (**C**) 1, (**F**) 3 and (**I**) 5. The grey line shows the theoretical line of no change in the grouping coefficient, while the black line is the line that best fits the observed data after the attacks. This figure shows results for dendrite no. 2; the complete set of results for each Tau- dendrite are shown in Supplementary Table 3. Means and standard deviations are computed over 100 random attacks.

## Discussion

The understanding of how spines are lost in AD is still unclear but could potentially reveal the mechanisms underlying synaptic damage in this disorder. In this study, we show that the presence of tau pathology in CA1 pyramidal neurons is associated with a distinct organization of spines into smaller and shorter communities. This reorganization is due to a specific pattern of spine loss in groups or blocks of spines in Tau+ dendrites. These findings indicate that the loss of spines associated with tau pathology is not a random process but occurs in clusters, shedding light onto the neurodegenerative changes that occur in the course of AD.

It is well established that the tau protein plays an important role in stabilizing microtubules and regulating axonal transport [21]. In addition to its role in supporting microtubules, tau also regulates other processes associated with synaptic function, being detected in the dendrites and the postsynaptic structures of healthy neurons [22-24]. In particular, tau can directly interact with scaffolding proteins, regulating the targeting of glutamatergic receptors to postsynaptic sites in spines. Moreover, there is evidence showing that tau is involved in long-term depression in the CA1 of the hippocampus [25, 26]. Overall, these studies suggest that tau exerts a central role controlling the normal healthy function of the synapses in the brain.

In AD, tau undergoes pathological changes such as hyperphosphorylation, which affect its affinity towards microtubules [27]. These changes eventually lead to the detachment of tau from microtubules, their translocation from axons to the somatodendritic compartment and spines, where it can interfere with synaptic function [28]. The modified tau molecules tend to self-assemble into paired helical filaments, which form neurofibrillary tangles that exert toxicity on the neuron [28], leading to neurodegenerative changes such as the loss of spines. In line with this, we have previously found a loss of spines in pyramidal neurons with tau pathology in AD patients [13]. Since generally one spine corresponds to one excitatory synapse [29], the loss of spines in pyramidal neurons with tau indicates they receive a lower number of excitatory inputs, reducing synaptic communication.

However, to this date, the mechanisms underlying spine loss in AD have not been investigated. In line with this, there is increasing evidence showing that

functionally related synapses are organized in clusters and that these clusters are crucial for cognitive functions that become impaired in AD such as memory storage and maintenance [9, 12]. This has led to the proposal of a hypothesis based on clustered plasticity, which supports the idea that the number and position of spines in the dendrites as well as their excitatory synapses depend on the dynamics of neuronal connectivity and that learning and memory can lead to the organization of spines in clusters [30, 31]. Thus, in this study we assess the spine organization in a unique dataset of dendrites with and without tau pathology from three AD cases. By modeling dendrites as graphs, where the spines represent nodes and the connections between the spines reflect how close they are to each other, we have found a specific change in the pattern of spine organization into communities in dendrites with tau pathology. To investigate the mechanisms responsible for this abnormal organization, we performed a series of simulated attacks to the dendrites without tau pathology. These attacks revealed that only by removing spines in clusters, the attacked Tau- dendrites show an organization similar to that of Tau+ dendrites. These findings are in line with previous studies showing that the organization of spines in clusters is biologically meaningful in healthy neurons [9–12]. Here, we extend these findings by confirming that this organization is also associated with pathological conditions such as AD. In particular, our results show that AD is associated with a loss of clusters of spines, which could be the mechanism by which tau drives synaptic damage in this disorder, leading the way to cognitive deficits.

With increasing recognition of AD as a synaptic disorder [32], maintaining the function of spines may become an important therapeutic target in the future. Our results suggest that when it comes to the normal organization of the dendrite, it is important to maintain the healthy function of clusters of spines rather than single spines, and thus new treatments should focus on preventing damage to these relevant functional units. In addition, recent clinical trials in sporadic and familial AD show that anti-amyloid drugs reduce the levels of phosphorylated tau, indicating that these treatments have downstream effects on tau metabolism and synaptic function [33]. Thus, assessing the organization of spines or developing in-vivo biomarkers that reflect the integrity of spine clusters within the dendrites will

become important to assess the clinical effects of these trials since synapses are crucial for memory and other cognitive functions that become impaired in AD.

Our approach of modeling the dendrites as a graph has several advantages. By integrating each spine in a network with all the other spines of the same dendrite, we can assess its architecture using topological measures that reflect the communities. These measures have been extensively applied to assess the organization of the brain in human individuals, revealing that normal brain function requires a network organization divided into communities, with potentially different functions or connectivity patterns [34, 35]. To our knowledge, our study is the first to apply a graph-theory approach to assess the organization of spines. This approach allowed us to establish that the random loss of spines is not responsible for the reorganization observed in dendrites with tau pathology. Instead, clusters of spines seem to play a key role in this reorganization, in line with previous studies using magnetic resonance imaging showing that groups of tightly connected brain regions are an important measure that becomes altered in patients with AD [36].

Our study has also a few limitations such as the lack of ante-mortem cognitive measures for the AD cases that we could have used to correlate with the loss of spine blocks and assess the clinical value of these changes in our sample. In addition, the lack of brain tissue from elderly individuals without AD would have been interesting to include in order to assess the organization of spines in normal brains, although normal brains are likely to have several other pathologies that could influence synaptic integrity [37].

In summary, this study shows that AD is associated with a reorganization of spines into smaller and more tightly packed communities due to a loss of groups of spines in dendrites with tau pathology. These findings suggest that tau targets spines in clusters along the dendrite, damaging synaptic connections that potentially share the same synaptic contact.

## MATERIALS AND METHODS

**Human brain samples**. In this study, we have used unpublished material from ref. [13]. Briefly, brain tissue from three AD patients was obtained at autopsy from the Instituto de Neuropatología (Dr I. Ferrer, Servicio de Anatomía Patológica,

IDIBELL-Hospital Universitario de Bellvitge, Barcelona, Spain), from the Banco de Tejidos Fundación CIEN (Centro Alzheimer, Fundación Reina Sofía, Madrid, Spain) and from the Neurological Tissue Bank (Biobanc-Hospital Clínic-IDIBAPS, Universidad de Barcelona, Spain). Following neuropathological examination, the pathological state (Supplementary Table 4) was defined according to the CERAD (*The Consortium to Establish a Registry for Alzheimer's Disease (CERAD) | Neurology*, n.d.) and the Braak and Braak criteria [38]. In all cases, the time between death and tissue fixation was 1.5–3 h, and the brain samples were obtained following the guidelines and with the approval of the Institutional Ethical Committee.

**Intracellular injections and immunocytochemistry**. Coronal sections (250 μm) were obtained with a vibratome and labeled with 4,6 diamino-2-phenylindole (DAPI; Sigma, St Louis, MO, USA) to identify cell bodies. Pyramidal cells from the CA1 region were then individually injected with LY (8% in 0.1 M Tris buffer, pH 7.4). LY was applied to each injected cell by continuous current until the distal tips of each cell fluoresced brightly, indicating that the dendrites were completely filled and ensuring that the fluorescence did not diminish at a distance from the soma. Following intracellular injections, sections were double-immunostained with anti-LY and either anti-PHF-tau$_{AT8}$ or anti-PHF-tau$_{PHF\text{-}1}$ antibodies [13]. We performed a total of 150 intracellular injections in CA1 pyramidal neurons (P9: 40 LY-Injected neurons; P13: 62 LY-Injected neurons; P14: 48 LY-Injected neurons). We then reconstructed the spines in three dimensions by confocal microscopy using a previously described methodology [39]. Only complete dendrites were included in the analysis.

**Construction of graphs**. We modeled each individual dendrite as a graph represented by a set of nodes and edges, where nodes represent the elements of the graph (dendritic spines) and the edges indicate the strength of association between these elements. In this model, the strength of association between the nodes is proportional to the physical closeness between the spines and is calculated as the inverse distance between the spines along the dendrite. Let $i$ and $k$ represent two spines along the dendrite, and let $S = i \rightarrow j \rightarrow a \rightarrow b \rightarrow \ldots \rightarrow$

$u \to v \to k$ denote the complete sequence of neighboring spines positioned between $i$ and $k$. For each pair of neighboring spines belonging to this sequence, e.g. $u$ and $v$ at positions $r_u = (x_u, y_u, z_u)$ and $r_v = (x_v, y_v, z_v)$ respectively, the distance between them is calculated as:

$$D_{uv} = \sqrt{(x_v - x_u)^2 + (y_v - y_u)^2 + (z_v - z_u)^2}$$

Since the distance between any pair of neighboring spines along the sequence $S$ is much smaller than the total length of the dendrite ($D_{uv} \ll L$), the total distance between $i$ and $k$ along the dendrite is represented as a sum of the distances between all consecutive pairs of spines within the sequence:

$$d_{ik} = \sum_{\substack{u,v \in S \\ u>v, u=v+1}} D_{uv}$$

Finally, the strength of association between spines $i$ and $k$ can be expressed as

$$w_{ik} = {}^{1}/_{d_{ik}}$$

After calculating the pairwise strength of association between all possible pairs of spines and the construction of the corresponding graph, various graph measures can be calculated in order to investigate its local and global organization. In our analysis, we focused on the global community organization of the dendrite by calculating the number of spines within each community as well as the characteristic community extension. In addition, we also calculated the total number of spines of each dendrite and the mean grouping coefficient.

**Community structure and characteristic community extension**. The community structure of a graph reflects how well the graph can be fragmented into different sub-graphs or communities. Communities are defined as groups of nodes that are tightly connected with each other but are poorly connected with nodes from other communities. Here, we calculate the community structure by using the Louvain algorithm [20], which optimizes the modularity of the graph by iteratively merging communities into single nodes and subsequently recalculating the modularity on the corresponding graph. Modularity is a measure that compares the density of within-community connections with that of a random graph; higher modularity values indicate a better division of the graph into communities. The modularity is calculated as:

$$m = \frac{1}{l}\sum_{ij}\left(A_{ij} - \frac{k_i k_j}{l}\right)\delta_{ij}$$

where $l$ is the number of edges in the graph, $A_{ij}$ is the adjacency matrix of the graph, $k_i$ ($k_j$) is the degree of the node $i$ ($j$), $\delta_{ij}$ is 1 if the two nodes belong to the same community and 0 otherwise, and the sum is performed over all pairs of nodes in the graph.

We define the characteristic community extension as the average distance between all pairs of spines that belong to the same community.

**Mean grouping coefficient**. For each spine, we quantified the degree to which that node is part of a tightly connected neighborhood. Given a set of three spines $i$, $j$ and $k$, let the connection strength between nodes $i$ and $j$ be represented as $w_{ij}$, between nodes $i$ and $k$ as $w_{ik}$, and between nodes $j$ and $k$ as $w_{jk}$. The weight of the triangle formed by these three connections can be expressed as:

$$T_{ijk} = w_{ij}^{1/3} w_{ik}^{1/3} w_{jk}^{1/3} = \frac{1}{d_{ij}^{1/3} d_{ik}^{1/3} d_{jk}^{1/3}}$$

where $d_{ij}$, $d_{ik}$ and $d_{jk}$ are the distances between the corresponding spines. The triangle weight $T_{ijk}$ reflects the positions of the three spines along the dendrite relative to each other. Therefore, small values of $T_{ijk}$ indicate that the three corresponding spines $i$, $j$ and $k$ are spaced far away from each other, while larger values indicate that the three spines are positioned closely to each other along the dendrite.

The mean grouping coefficient for the spine $i$ is the average weight of all triangles the spine $i$ is part of, and it characterizes the position of spine $i$ in the dendrite relative to all other spines. This coefficient ranges between 0 and 1, where 1 is calculated for spines that are part of a tight neighborhood with many spines positioned nearby. Conversely, spines with a coefficient of 0 belong to a spread-out neighborhood and are as far as possible from the other spines. We calculated this coefficient as:

$$GC_i = \frac{(1/2)\sum_{j\neq i}\sum_{h\neq(i,j)} T_{ijk}}{(1/2)(N-1)(N-2)} = \frac{(1/2)\sum_{j\neq i}\sum_{h\neq(i,j)} w_{ij}^{1/3} w_{ih}^{1/3} w_{jh}^{1/3}}{(1/2)(N-1)(N-2)},$$

where $N$ is the number of spines along the dendrite to which $i$ belongs to.

**Statistical comparison of the results**. Differences between Tau+ and Tau- dendrites were assessed using non-parametric permutation tests with 10 000 permutations, which were considered significant for a two-tailed test of the null hypothesis at $p<0.05$ [40]. The tests were performed by first calculating the difference in the means between the two groups. Then, we randomly permuted the elements from both groups and calculated the differences in the means between the new randomized groups. By repeating this procedure multiple times, we obtained a null distribution of between-group differences. Finally, we obtained the two-tailed p-value as the proportion of between-group differences in the null distribution that are greater than the absolute value of the original difference. The community structure parameters were obtained as averages of 100 trials.

## Disclosures

The authors declare that the research was conducted in the absence of any commercial or financial relationships that could be construed as a potential conflict of interest.

## Acknowledgements

This work was supported by grants from the Spanish Ministerio de Ciencia, Innovación y Universidades (grant IJCI-2016-27658 to PMS, grant PGC2018-094307-B-I00), the Cajal Blue Brain Project (the Spanish partner of the Blue Brain Project initiative from EPFL, Switzerland) and the Centro de Investigación Biomédica en Red sobre Enfermedades Neurodegenerativas (CIBERNED, CB06/05/0066, Spain). JBP is currently supported by grants from the Swedish Research Council (#2018-02201), Hjärnfonden (#FO2019-0289), Alzheimerfonden (#AF-930827) and the Strategic Research Programme in Neuroscience at Karolinska Institutet (Stratneuro Startup Grant). We would like to thank Carmen Álvarez and Lorena Valdés for their helpful assistance.

## Data sharing

Anonymized data will be shared by request from a qualified academic investigator for the sole purpose of replicating procedures and results presented in the article.

## Author contributions

P.M.S., J.D., I.F., J.B.P. and G.V. conceptualized the study. P.M.S., J.D., I.F. performed the intracellular injections and immunocytochemistry analyses. M.M. performed the graph and statistical analyses. All authors contributed to drafting, reviewing and editing the manuscript.

## References

[1] Winblad B. et al. Defeating Alzheimer's disease and other dementias: a priority for European science and society. *The Lancet Neurology*, **15**(5), 455-532 (2016).

[2] Edwards F.A. A unifying hypothesis for Alzheimer's disease: from plaques to neurodegeneration. *Trends in Neurosciences* **42**(5), 310-22 (2019).

[3] Spruston N. Pyramidal neurons: Dendritic structure and synaptic integration. *Nature Reviews Neuroscience* **9**(3), 206–221 (2008).

[4] DeFelipe, J. The dendritic spine story: An intriguing process of discovery. *Frontiers in Neuroanatomy* **9**, 14 (2015).

[5] Kandel E. R., Dudai Y. & Mayford M. R. The molecular and systems biology of memory. *Cell* **157**(1), 163–186 (2014).

[6] Yuste R. *Dendritic Spines*. (MIT Press, Cambridge (MA), 2010).

[7] Eyal G. et al. Human cortical pyramidal neurons: from spines to spikes via models. *Frontiers in Cellular Neuroscience* **12, 181** (2018).

[8] Winnubst J. & Lohmann C. Synaptic clustering during development and learning: the why, when, and how. *Frontiers in Molecular Neuroscience* **5**, 70 (2012).

[9] Branco T., & Häusser M. Synaptic integration gradients in single cortical pyramidal cell dendrites. *Neuron* **69**(5), 885–892 (2011).

[10] Govindarajan A., Kelleher R. & Tonegawa, S. A clustered plasticity model of long-term memory engrams. *Nature Reviews Neuroscience* **7,** 575–583 (2006).

[11] Wen Q., Stepanyants A., Elston G.N., Grosberg A.Y., & Chklovskii, D.B. Maximization of the connectivity repertoire as a statistical principle governing the shapes of dendritic arbors. *Proceedings of the National Academy of Sciences U.S.A.* **106**(30), 12536–12541 (2009).

[12] Kastellakis G., Cai D.J., Mednick S.C., Silva A.J., & Poirazi P. Synaptic clustering within dendrites: An emerging theory of memory formation. *Progress in Neurobiology* **126**, 19–35 (2015).

[13] Merino-Serrais P. et al. The influence of phospho-tau on dendritic spines of cortical pyramidal neurons in patients with Alzheimer's disease. *Brain* **136**(6), 1913–1928 (2013).

[14] Lu J. & Zuo Y. Clustered structural and functional plasticity of dendritic spines. *Brain Research Bulletin* **129**, 18-22 (2017).

[15] Avila J. et al. Tau phosphorylation by GSK3 in different conditions. *International Journal of Alzheimer's Disease* **2012**, 1–7 (2012).

[16] Grundke-Iqbal I. et al. Abnormal phosphorylation of the microtubule-associated protein tau (tau) in Alzheimer cytoskeletal pathology. *Proceedings of the National Academy of Sciences U.S.A.* **83**(13), 4913–4917 (1986).

[17] Knafo S. et al. Widespread changes in dendritic spines in a model of Alzheimer's disease. *Cerebral Cortex* **19**(3), 586–592 (2009).

[18] Spires T. L. et al. Dendritic spine abnormalities in amyloid precursor protein transgenic mice demonstrated by gene transfer and intravital multiphoton microscopy. *Journal of Neuroscience* **25**(31), 7278–7287 (2005).

[19] Tsai J., Grutzendler J., Duff K., & Gan W.-B. Fibrillar amyloid deposition leads to local synaptic abnormalities and breakage of neuronal branches. *Nature Neuroscience* **7**(11), 1181–1183 (2004).

[20] Blondel V.D., Guillaume J.-L., Lambiotte R. & Lefebvre E. Fast unfolding of communities in large networks. *Journal of Statistical Mechanics: Theory and Experiment* **2008**(10), 10008 (2008).

[21] Wang Y. and Mandelkow E. Tau in physiology and pathology. *Nature Reviews Neuroscience* **17**(1), 22 (2016).

[22] Liao D., Miller E.C. & Teravskis, P.J. (2014). Tau acts as a mediator for Alzheimer's disease-related synaptic deficits. *European Journal of Neuroscience* **39**(7), 1202-1213 (2014).

[23] Pooler A.M., Noble W. & Hanger D.P. A role for tau at the synapse in Alzheimer's disease pathogenesis. *Neuropharmacology* **76**, 1-8 (2014).

[24] Regan P., Whitcomb D.J. & Cho, K. Physiological and pathophysiological implications of synaptic tau. *The Neuroscientist* **23**(2), 137-151 (2017).

[25] Kimura T. et al. Microtubule-associated protein tau is essential for long-term depression in the hippocampus. *Philosophical Transactions of the Royal Society B: Biological Sciences* **369**(1633), 20130144 (2014).

[26] Regan P. et al. Tau phosphorylation at serine 396 residue is required for hippocampal LTD. *Journal of Neuroscience* **35**(12), 4804-4812 (2015).

[27] Arendt T., Stieler J.T. & Holzer, M. Tau and tauopathies. *Brain Research Bulletin* **126**, 238-292 (2016).

[28] Forner S. et al. Synaptic impairment in Alzheimer's disease: a dysregulated symphony. *Trends in Neurosciences* **40**(6), 347-357 (2017).

[29] Arellano J.I., Benavides-Piccione R., DeFelipe J. & Yuste R. Ultrastructure of dendritic spines: correlation between synaptic and spine morphologies. *Frontiers in Neuroscience* **1**, 10 (2007).

[30] Frank A.C. et al. Hotspots of dendritic spine turnover facilitate clustered spine addition and learning and memory. *Nature Communications* **9**(1), 422 (2018).

[31] Fu M., Yu X., Lu J. & Zuo Y. Repetitive motor learning induces coordinated formation of clustered dendritic spines in vivo. *Nature* **483**(7387), 92–95 (2012).

[32] Bereczki E. et al. Synaptic markers of cognitive decline in neurodegenerative diseases: a proteomic approach. *Brain* **141**(2), 582-95 (2018).

[33] Tolar M., Abushakra S., Hey J.A., Porsteinsson A. & Sabbagh M. Aducanumab, gantenerumab, BAN2401, and ALZ-801—the first wave of amyloid-targeting drugs for Alzheimer's disease with potential for near term approval. *Alzheimer's Research & Therapy* **12**(1), 1-10 (2020).

[34] Shen X., Papademetris X., Constable R.T. Graph-theory based parcellation of functional subunits in the brain from resting-state fMRI data. *Neuroimage* **50**(3), 1027-35 (2010).

[35] Meunier D., Lambiotte R., Bullmore E.T. Modular and hierarchically modular organization of brain networks. *Frontiers in Neuroscience* **4,** 200 (2010).

[36] Pereira J.B. et al. Disrupted network topology in patients with stable and progressive mild cognitive impairment and Alzheimer's disease. *Cerebral Cortex* **26**(8), 3476-93 (2016).

[37] Kovacs G.G. et al. Non-Alzheimer neurodegenerative pathologies and their combinations are more frequent than commonly believed in the elderly brain: a community-based autopsy series. *Acta Neuropathologica* **126**(3)**,** 365-84 (2013).

[38] Braak H., & Braak E. Demonstration of amyloid deposits and neurofibrillary changes in whole brain sections. *Brain Pathology* **1**(3), 213–216 (1991).

[39] Benavides-Piccione R., Fernaud-Espinosa I., Robles V., Yuste R., & DeFelipe, J. Age-based comparison of human dendritic spine structure using complete three-dimensional reconstructions. *Cerebral Cortex* **23**(8), 1798–1810 (2013).

[40] He Y., Chen Z. & Evans A. Structural insights into aberrant topological patterns of large-scale cortical networks in alzheimer's disease. *Journal of Neuroscience* **28**(18)**,** 4756-4766 (2008).